Numerical Prediction of Air-preheating Effect on Soot Formation in Diffusion Flame During Early Transience Following Ignition

Bijan Kumar Mandal, Amitava Datta, and Amitava Sarkar

Abstract— **A CFD-based numerical model has been developed for the determination of the volume concentration and number density of soot in a laminar diffusion flame of methane in air, under transient condition following ignition of the flame. The transience is studied from the point of ignition till the final steady state is reached. The burner is an axi-symmetric co-flowing one with the fuel issuing through a central port and air through an annular port. The air is considered to be without and with preheat. Attention is focused on various soot forming and destruction processes, like nucleation, growth and oxidation, during the transient phase to evaluate their relative importance. The contribution of surface growth towards soot formation is more significant than that of nucleation during the early periods following ignition. Once the high temperature reaches the oxygen-enriched zone beyond the flame, the soot oxidation becomes important. Coagulation, on the other hand, limits the soot particle number. Preheating of air increases the soot volume fraction in the steady flame significantly. However, there is not much difference in the qualitative development of the soot-laden zone during the flame transient period.**

***Index Terms*—air preheating, laminar diffusion flame, oxidation, soot, Transient modeling**

I. Introduction

Soot is an atmospheric pollutant formed in hydrocarbon combustion, which causes respiratory illness and increases mortality. Soot in flame results from incomplete combustion of hydrocarbons in the reducing atmosphere, where enough oxygen is not available to yield a complete conversion of fuel to carbon di-oxide and water vapour. Soot particles in flame also play a major role in heat transfer from the flame. Therefore, better understanding and control of soot forming processes in hydrocarbon combustion are required.

Manuscript received March 13, 2007.

Bijan Kumar Mandal is with the Mechanical Engineering Department, Bengal Engineering and Science University, Shibpur, Howrah 711 103, India (phone: 91 033 26887619; fax: 91 033 26684561; e-mail: bkm375@yahoo.co.in).

Amitava Datta is with the Department of Power Engineering, Jadavpur University, Salt Lake Campus, Kolkata 700098, India (e-mail: amdatta@hotmail.com).

Amitava Sarkar is with the Mechanical Engineering Department, Jadavpur University, Kolkata 700 032, India (e-mail: stutul@rediffmail.com).

Non-premixed or diffusion flames are sooty in nature. Practical diffusion flames are mostly turbulent, however, the study of laminar diffusion flames still finds importance because of their fundamental nature and due to the fact that the turbulent diffusion flames can be taken as an aggregate of laminar flamelets. Wey *et al.* [1], Santoro *et al*. [2], Smooke *et al.* [3] and Lee *et al.* [4] performed experiments in laminar diffusion flames using various hydrocarbon fuels for the determination of soot. Different semi-empirical models of soot formation, based on simple description of soot chemistry, have been developed by Smith [5], Gore and Faeth [6], Kennedy *et al.* [7], Leung *et al.* [8] and Said *et al.* [9]. Syed *et al.* [10] considered surface growth to be a function of the aerosol surface area, while Moss *et al.* [11] took it to be dependent on number density. Oxidation of soot is another important issue, which controls its emission level. Two widely used oxidation models are due to Lee *et al.* [12] and Nagle and Strickland-Constable [13].

Almost all the works on soot production in laminar diffusion flames have been done on steady diffusion flames under different operating conditions and fuels. In turbulent diffusion flames local extinction and re-ignition of flame is observed, on which not much work has yet been done. The soot formation behaviour in the flame can be entirely different during flame development in a mixture following ignition compared to that in a steady flame. Not much work has yet been done on this aspect and therefore, the topic needs attention. Other transient flame applications, e.g. during lighting up of a burner flame and flame development in a diesel engine, are available where the flame is not steady and the behaviour can only be explained by doing a transient modeling of the flame development and pollutant formation.

With this motivation, soot formation during the transient development phase of a confined, co-flowing, laminar jet diffusion flame following ignition has been studied numerically in the present work. Methane is considered to be the fuel and the choice is made because it constitutes more than 90% of natural gas. The soot models of Syed *et al.* [10] and Moss *et al.* [11] are employed with the necessary adjustments for the sake of compatibility with the present combustion model. Governing equations for soot volume fraction and number density are solved along with the equations of mass, momentum, energy and gas phase species concentrations. The

radiative energy transport in the flame is neglected. Effect of air preheating on soot formation has also been studied under transient condition.

II. Model formulation

A. Reacting Flow Model

An axi-symmetric laminar diffusion flame in a confined physical environment is considered with fuel admitted as a central jet and air as a co-flowing annular jet. The inner fuel tube diameter is 12.7 mm and the outer tube diameter is 50.4 mm. The combustion process is simulated with a detailed numerical model, which is developed for solving the transient governing equations for a laminar, reacting flow with appropriate boundary conditions along with the formation of soot. The conservation equations for mass and momentum, energy and species are same as described in the earlier work of Mandal *et al.* [14]. The combustion reaction of methane and air is assumed to proceed through a simplified two steps global reaction chemistry. The specific heat is a strong function of temperature and is locally calculated for each species at the respective temperature. The mixture specific heat is then calculated considering an ideal gas mixture. The temperature of the gas mixture is implicitly calculated from enthalpy. The transport of momentum, energy and species mass in the calculation of a reacting flow involve the transport coefficients like viscosity, thermal conductivity and mass diffusivity for the solution. The local variation of viscosity, thermal conductivity and mass diffusivity with temperature has also been taken into consideration.

B. Soot Formation Model:

The formation of soot is modeled in the line prescribed by Syed *et al.* [10] and Moss *et al*. [11]. The soot volume fraction (f_v) and number density (n) are considered to be the important variables. Nucleation, surface growth, coagulation and oxidation effects are taken into account in the formation of the model equations. Following Syed *et al.* [10], the surface growth rate is evaluated considering the surface area of the soot particles into account. The soot oxidation (ω_{ox}) is calculated using the model of Lee *et al.* [12] and is accounted in the equation for volume fraction as was done by Moss *et al.* [11]. The conservation equations are formed for soot mass concentration ($\rho_s f_v$) and number density (as n/N_0) and the respective source terms for the conservation equations are as follows:

$$\frac{d}{dt}\left(\rho_s f_v\right) = \gamma\left(\rho_s f_v\right)^{2/3} n^{1/3} + \delta - \left(\frac{36\pi}{\rho_s^2}\right)^{1/3}\left(n\rho_s^2 f_v^2\right)^{1/3}\omega_{ox} \tag{1}$$

$$\frac{d}{dt}\left(\frac{n}{N_0}\right) = \alpha - \beta\left(\frac{n}{N_0}\right)^2 \tag{2}$$

where,

$$\alpha = C_\alpha \rho^2 T^{0.5} X_c \exp\left(-\frac{T_\alpha}{T}\right)$$

$$\beta = C_\beta T^{0.5}$$

$$\gamma = C_\gamma \rho T^{0.5} X_c \exp\left(-\frac{T_\gamma}{T}\right)$$

$$\delta = C_\delta \alpha$$

In the above equations, N_0 is Avogadro number, ρ_s is the soot particulate density (=1800 kg/m^3), T_α and T_γ are activation temperatures for nucleation and growth, respectively, C_α , C_β, C_γ , C_δ are model constants and ρ and T are the local mixture density and temperature, respectively. The model constants and activation temperatures are taken from Syed *et al.* [10], for methane fuel. In the work of Syed *et al.* and Moss *et al.*, X_c was referred as the mole fraction of the parent fuel species.

In (1), the first and second terms on the right hand side are the contributions of the soot surface growth and soot nucleation respectively, while the third term pertains to the depletion of soot due to oxidation. The terms on the right hand side of (2) are due to the contribution of nucleation and coagulation, respectively. The nucleation and surface growth terms account for the chemical phenomena through Arrhenius type rate equation. The coagulation term is derived from the Smolushowski equation for coagulation of liquid colloids.

Conservation equations for the soot mass concentration and number density are solved in the present model along with the gaseous species in the solution domain. As soot particles do not follow the molecular diffusion theory, the diffusion velocities in the soot conservation equations are replaced by the corresponding thermophoretic soot particle velocities. Therefore, the conservation equations, in general, can be expressed

$$\frac{\partial \varphi}{\partial t} + \frac{1}{r}\frac{\partial}{\partial r}\left(r v_r \varphi\right) + \frac{\partial}{\partial z}\left(\rho v_z \varphi\right) = \frac{1}{r}\frac{\partial}{\partial r}\left(r V_{t_r} \varphi\right) + \frac{\partial}{\partial z}\left(V_{t_z} \varphi\right) + \dot{S}_\varphi \tag{3}$$

The above equation is applicable both for the soot mass concentration ($\rho_s f_v$) and number density (n/N_0) and accordingly ϕ will assume the respective variable value. The thermophoretic velocity vector (V_t) has been calculated following Santoro *et al.* [2] as

$$V_t = \frac{3}{4\left(1+\pi\xi/8\right)}\frac{\upsilon}{T}\nabla T \tag{4}$$

where, the accommodation factor (ξ) has been taken as unity.

Equations (1) and (2) form the source terms ($\dot{S}_\varphi$) of the conservation equations of the soot mass concentration and number density, respectively. The soot volume fraction is obtained from the mass concentration solution.

III. Numerical Scheme

The gas phase conservation equations of mass, momentum, energy and species concentrations along with the conservation equations of soot mass concentration and number density are solved simultaneously, with their appropriate boundary conditions, by an explicit finite difference computing technique taking into account the transient terms in the equations. The variables are defined following a staggered grid arrangement. The advection terms are discretised following a hybrid-differencing scheme, based on cell Peclet number, while the diffusion terms are discretised by the central differencing scheme. The solution is explicitly advanced in time satisfying the condition that a fluid particle should never cross a complete cell, in either direction, in one time step. In every time step, first the axial and radial momentum equations are solved. Pressure corrections and the associated corrections of velocities to satisfy the conservation of mass are then done by an iterative scheme. The enthalpy transport and the species transport equations, including those of soot variables, are subsequently solved within the same time step. The temperature is decoded from the enthalpy and species concentration values by Newton-Raphson method. Transient results at desired intermediate times are achieved in the process of time advancement. The process continues till a steady state convergence is reached.

Boundary conditions at the inlet are given separately for the fuel stream at the central jet and the air stream at the annular co-flow. No soot is considered to enter with the flow through the inlet plane. Considering the length of the computational domain to be 0.3 m, the fully developed boundary conditions for the variables are considered at the outlet. In case of reverse flow at the outlet plane, which occurs in the case of buoyant flame, the stream coming in from the outside is considered to be atmospheric air. Axi-symmetric condition is considered at the central axis, while at the wall a no-slip, adiabatic and impermeable boundary condition is adopted.

A variable size adaptive grid system is considered with higher concentration of nodes near the axis. An extensive grid independence test has been carried out by several variations of the number of grids in either direction. Finally an optimal numerical mesh with 85×41grid nodes is finally adopted considering the accuracy as well as the computation time.

IV. Results and Discussion

A. Validation of the Numerical Code

The numerical code for the reacting flow is validated by comparing the predictions against experiments conducted by Mitchell *et al.* [15]. The soot model employed in the present work is calibrated against the experimental results of Smooke *et al.* [3] for the same burner configuration and input conditions. We have compared the soot volume fraction described by the present model against the experiments of Smooke *et al.* at the same non-dimensional axial height z/H_F, where H_F is the flame height. Fig.1 shows the radial distributions of the soot volume fraction at two axial positions inside the flame. The figures reveal that the present code is capable of predicting the soot distribution quite well.

B. Soot Distribution in Transient Flame

In our earlier work [14], we discussed elaborately the transient development of a diffusion flame from a co-flow burner having the same configuration as in the present case. The main interest of the present work is to look into the distribution of soot particle concentration during the transient development of the flame, at different time planes, after ignition. Fig. 2 shows the distributions of soot volume fractions along with the flame contour at different times. The objective here is to observe how the various soot related processes play their roles to control the formation, growth and oxidation of the soot particles at different positions of the flame till the steady state is reached. It is seen in the Fig. 2a that though a thin flame is established 0.05 s after the

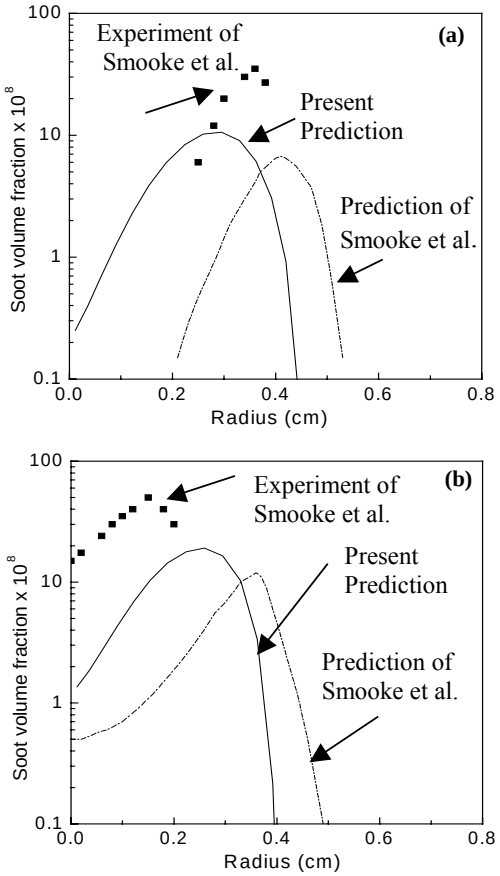

Fig. 1. Radial distribution of soot volume fraction in diffusion flame at non-dimensional axial heights (a) z/H_F = 0.5, (b) z/H_F = 0.69: Comparison of the present prediction against Smooke *et al.* [3].

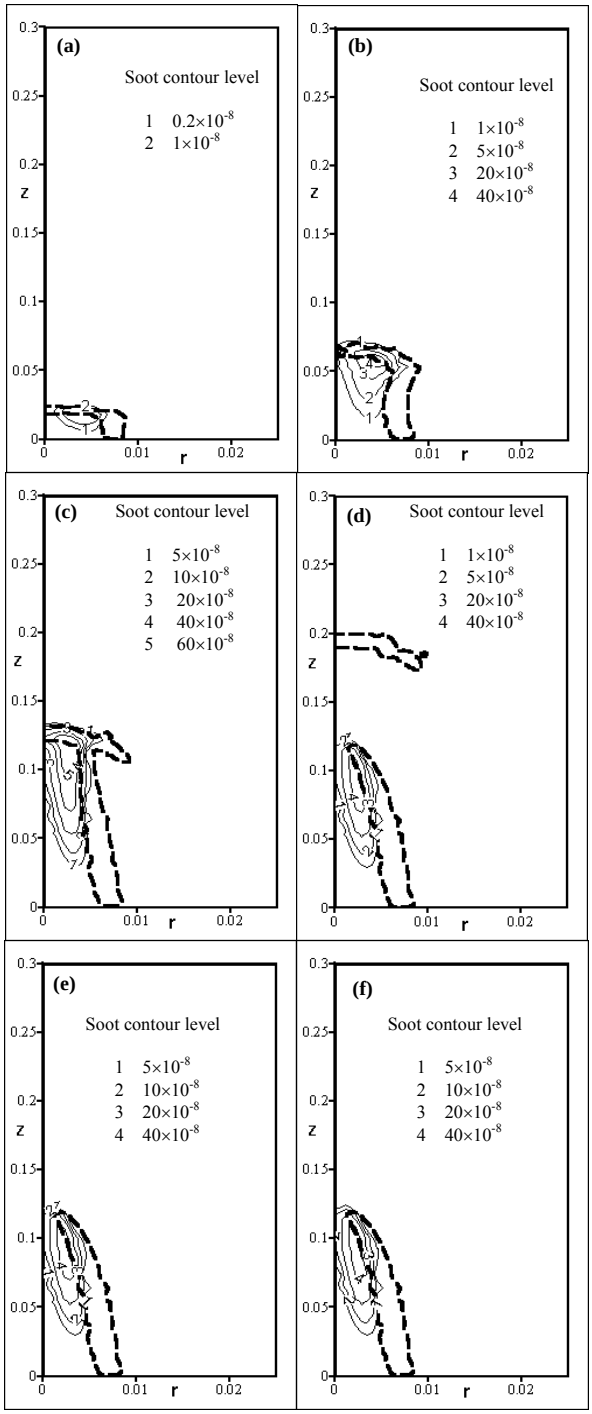

Fig. 2. Flame front surface (thick dotted line) and soot volume fraction contours at different times after ignition for a co-flowing jet diffusion flame (fuel inlet temp. = 300 K and air inlet temp. = 300 K): (a) t = 0.05 s, (b) t = 0.10 s, (c) t = 0.15 s, (d) t = 0.20 s, (e) 0.4 s, (f) 0.8 s.

ignition is given, the soot volume fraction is very low. This is because the temperature in the flame is relatively less and the time is also too short to cause a significant nucleation or growth of the soot particles. It is observed that the soot formation in a methane diffusion flame hardly initiates below a threshold temperature, which is about 1300 K. With the passage of time, the soot formation process accelerates with the increase in the rate of nucleation and growth. The increase in temperature plays a major role in achieving this. At 0.1 s, the maximum soot volume fraction reaches a value of 60×10^{-8}. A high contour value of 40×10^{-8} occurs inside the flame (Fig. 2b). The high soot concentration zone is observed inside the flame surface because of the high fuel concentration there. Beyond the flame, the soot particles are oxidized due to the presence of oxygen at high temperature. As the flame develops with time and elongates downstream, the soot-containing zone also shifts axially above the burner tip. The maximum soot volume fraction at 0.15 s after ignition is 120×10^{-8}, which is much more than the peak values of the earlier time. A high soot concentration contour of 60×10^{-8} is shown in Fig. 2c. Subsequent to this time, the peak soot concentration falls and at 0.2 s (Fig. 2d) the highest soot volume fraction is 67×10^{-8}. The higher soot formation during the earlier time was due to the accumulated fuel in the chamber that remained unburnt due to the absence of the flame front surface. Once the accumulated fuel is burnt, conditions tend towards the steady state and maximum soot volume fraction comes down. This fact is further augmented by the increase in soot oxidation. Another observation from the Fig. 2 is that the soot intensive zone, having the maximum soot volume fractions, shifts radially towards the axis with time. Interestingly, the second flame, observed at this time (t = 0.2 s), is found to be non-sooty. This is because the burning of the escaped fuel takes place in the premixed mode as it gets time to mix with the entrained oxygen. The soot distributions at 0.4 and 0.8 s after ignition are similar. The flame reaches its steady state before 0.4 s, and the transience in the domain continues till 0.8 s only because of adjustments above the flame region. The soot formation primarily occurs inside the flame region. Therefore, the soot distribution does not change much once the flame becomes stable.

Fig. 3a and Fig. 3b show the variation of the total soot volume and cumulative soot particle number within the solution domain with time measured from the point of ignition. It is observed from the figures that both the soot volume and soot particle number first increase to reach a peak and subsequently decrease and finally reach a steady value. However, the times at which the two quantities reach their peak values are different. Initially, both nucleation and surface growth of the soot are important. However, results from the Fig. 3a and Fig. 3b reveal that the rate of increase of soot volume is greater than that of the soot particle number. This indicates that surface growth, and not nucleation, contributes significantly towards the soot formation process during the early period. The activation temperature for the surface growth process ($T_\gamma = 12.6\times10^3$) is lower than that of soot nucleation ($T_\alpha = 46.1\times10^3$). Therefore, when the gas temperature is low, the contribution of the surface growth towards the increase in soot volume fraction outweighs that of soot nucleation. As the temperature increases, the rate of nucleation increases more rapidly compared to the increase in the rate of surface growth. Furthermore, during the early period of soot formation, the size of the soot particles remains small and average surface area per unit volume of soot particle is large. The surface growth rate depends upon the available surface area of the soot particles,

and larger surface area results in faster surface growth during the initial period. After 0.15 s, a

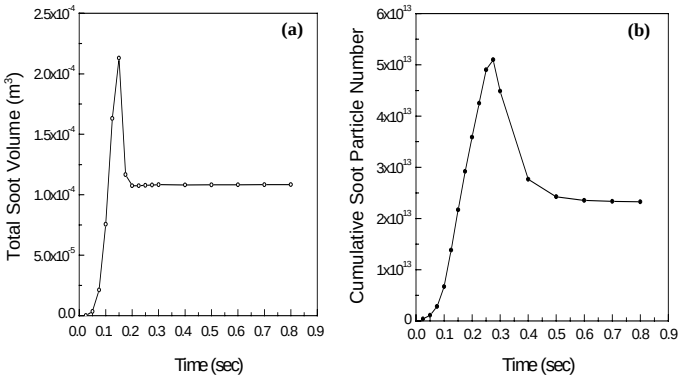

Fig. 3. Variation of (a) total soot volume, (b) cumulative soot particle number in the computational domain with time after ignition for the diffusion flame with fuel inlet temp. = 300 K and air inlet temp. = 300 K.

high temperature is found and soot oxidation takes a very important role. Though the number of soot particles increases due to further nucleation, but oxidation overcomes the surface growth to cause a decrease in the total soot volume. The soot surface growth is a function of the aerosol area and with the formation of more soot particles surface growth rate increases. It finally equals the soot oxidation rate and soot volume reaches a steady value. When many soot particles are formed in the domain, coagulation plays a major part. This is because coagulation is directly proportional to the square of the soot number density. Coagulation does not change the soot volume in the domain but reduces the number of particles within it. Finally, all the processes attain a state such that both the total soot volume and aggregate soot particle number reach their steady values.

C. Effect of Air Preheat on Soot formation

The effect of air preheating on soot formation has been studied by increasing the temperature of co-flowing air from 300 K to 400 K. First the steady state soot distribution due to air preheat has been looked into and then the transient development under this situation is discussed. The complete steady state in the whole domain is attained 3.2 s after the ignition is first given. The changes in the flame and flow characteristics play a major role on the soot formation process due to air preheating. A detailed discussion on the change in the flow pattern and temperature distribution without and with preheat in the present flame condition was presented in Mandal *et al*. [14]. The recirculating zone, which is formed without preheat is not realized now. More uniformity in the temperature distribution is obtained with the preheated air. Fig. 4a and Fig.4b show the centerline temperature and axial velocity distributions, respectively, without and with air preheat to clearly depict the differences in the central region. These differences in the conditions without and with preheat affects the soot formation processes in the flame.

Fig. 5 illustrates the flame front and the distribution of soot volume fraction in the flame with preheated air under steady condition. An over-ventilated flame structure with an open tip is obtained, similar to that without air preheat. But, a major difference is observed in the soot volume fraction. Though the soot-laden zone is again observed within the flame, the soot

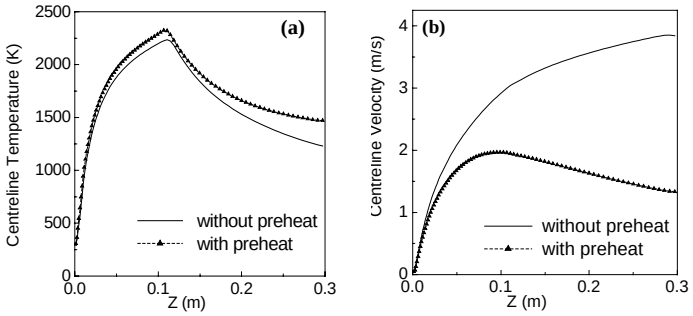

Fig. 4. (a) Centreline temperature, (b) centerline velocity distribution for the diffusion flame with and without air-preheat.

increase in the soot loading with air preheat can be attributed to the increase in flame temperature and the residence time of the gas in the flame core. The maximum soot volume fraction reaches a value more than 5 times of that without air preheat.

The development of the soot profile during the transient development of the flame and flow does not show much qualitative difference from the non-preheat case. When preheating of air is done, the complete steady state is attained after a much-prolonged time, mainly because of the complex post-flame transport processes. Therefore, though the flame front does not reflect any change 0.4 s after ignition, another 2.8 s is required to reach the final steady condition. Fig. 6 illustrates the soot volume fraction distributions at some intermediate times of 0.1 s, 0.2 s, 0.4 s and 1.6 s after the ignition, respectively. It is clearly evident from the figures that the qualitative trends remain similar to that without preheat of air.

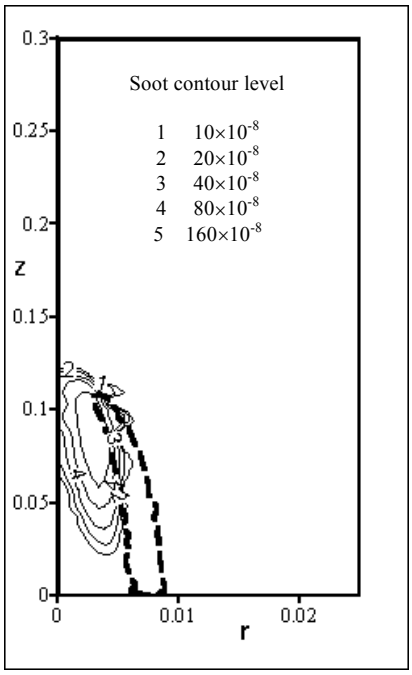

Fig. 5. Flame front (dashed thick line) and soot volume fraction contours with preheated air under steady state.

The only difference is in the magnitude of the soot volume fraction, which has remained more under all the corresponding times. The flame at 0.1 s (Fig. 6a) shows a diverging nature first before the rapid inward turn near the tip. The soot concentration is high in the core of the flame. But near the flame tip the concentration drops very rapidly. The flame at 0.2 s (Fig. 6b) is highly irregular owing to the flow pattern. The soot loading has increased much compared to the earlier time shown. At 0.4 s (Fig. 6c), an over-ventilated steady flame structure is arrived, with a small tip opening. The soot loading remains almost the same as in the previous time. As the soot formation takes place within the flame core and the soot oxidizes quite rapidly beyond the flame surface, not much change in the qualitative soot profiles are observed in the following times as well. However, a little change in the soot volume fraction value is noted. At 1.6 s, the soot volume fraction increases marginally (Fig. 6d). Since this time, not much change is observed even in the quantitative value of the volume fraction till the final steady state at 3.2 s.

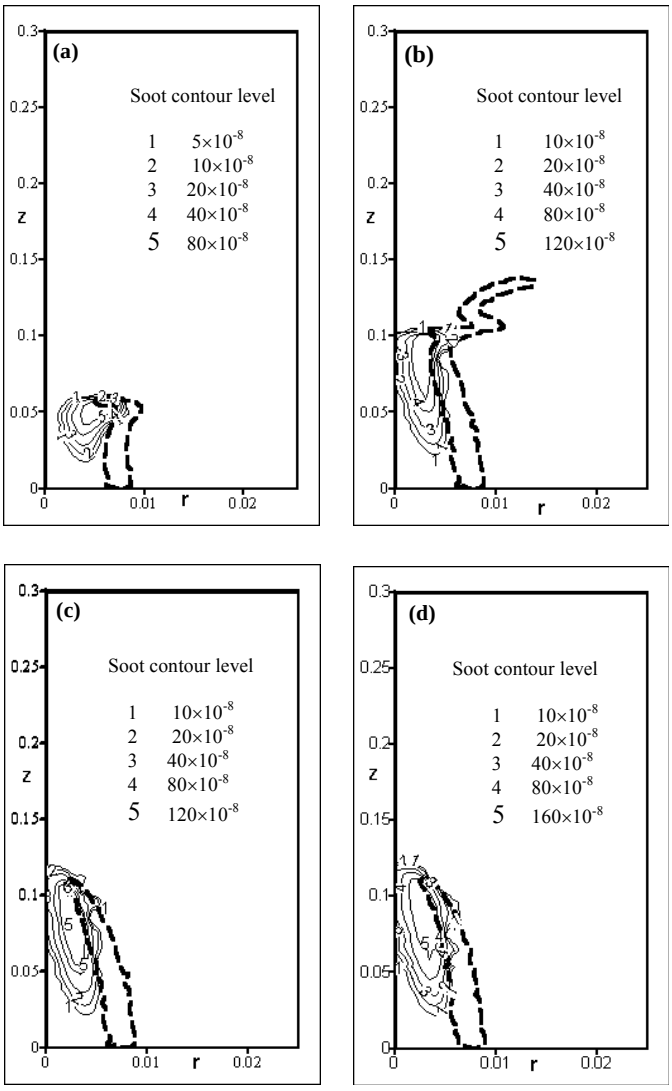

Fig. 6. Flame front (thick dotted line) and soot volume fraction contours at various times after ignition for diffusion flame with preheated air: (a) t = 0.10 s, (b) t = 0.20 s, (c) t = 0.40 s, (d) t =1.60 s.

REFERENCES

[1] C. Wey, E.A. Powell, and J.I. Jagoda, "The effect of temperature on the sooting behaviour of laminar diffusion flames," *Combustion Science and Technology*, vol. 41, 1984, pp. 173-190.

[2] R.J. Santoro, T.T. Yeh, J.J. Horvathand, and H.G. Semerjian, "The transport and growth of soot particles in laminar diffusion flames," *Combustion Science and Technology*, vol. 53, 1987,pp. 89 - 115.

[3] M.D.Smooke, C.S. McEnally, L.D. Pfefferle, R.J. Hall, and M.B. Colket, , "Computational and experimental study of soot formation in a coflow, laminar diffusion Flame," *Combustion and Flame*, vol. 117, No. 1-2, 1999, pp. 117- 139.

[4] K.O. Lee, C.M. Megaridis, S. Zelepouga, A.V. Saveliev, L.A. Kennedy, O. Charon, and F. Ammouri, "Soot formation effects of oxygen concentration in the oxidizer stream of laminar co-annulur non-premixed methane/air flames," *Combustion and Flame*, vol. 121, No. 1-2, 2000, pp. 323 - 333.

[5] G.M. Smith, "A simple nucleation/depletion model for the spherule size of particulate carbon," *Combustion and Flame*, vol. 48, 1982, pp. 265 - 272.

[6] J.P. Gore, and G.M. Faeth, Proceedings *of the Combustion Institute*, vol. 21, 1986, pp. 1521-1531.

[7] I.M. Kennedy, W. Kollmann, and J.Y. Chen, "A model for the soot formation in laminar diffusion flame," *Combustion and Flame*, vol. 81, No. 1, 1990, pp. 73 - 85.

[8] K.M Leung, R.P. Lindstedt, and W.P. Jones, "A simplified reaction mechanism for soot formation in non-premixed flames," *Combustion and Flame*, vol. 87, No. 3-4, 1991, pp. 289 - 305.

[9] R. Said, A. Garo, and R, Borghi, "Soot formation modeling for turbulent flames," *Combustion and Flame*, vol. 108, No. 1-2, 1997, pp. 71 - 86.

[10] K.J. Syed, C.D. Stewart, and J.B. Moss, ".Modelling soot formation and thermal radiation in buoyant turbulent diffusion flames," *Proceedings Combustion Institute*, vol. 23, 1990, pp. 1533-1539.

[11] J.B. Moss, C.D. Stewart, and K.J.Young, (1995) "Modelling soot formation and burnout in a high temperature laminar diffusion flame burning under oxygen-enriched conditions," *Combustion and Flame*, vol. 101, No. 4, 1995, pp. 491 - 500.

[12] K.B. Lee, M.W. Thring, and J.M. Beer, (1962), "On the rate of combustion of soot in a laminar soot flame," *Combustion and Flame*, vol. 6, 1962, pp. 137 - 145.

[13] J. Nagle, and R.F. Strickland-Constable, *Fifth Carbon Conf*., Vol. 1, 1962, pp. 154-164.

[14] B.K. Mandal, A. Datta, and A. Sarkar (2005) "Transient development of methane-air diffusion flame in a confined geometry with and without air-preheat," *International Journal for Energy Research*, vol. 29, No. 2, 2005, pp. 145-176.

[15] R.E. Mitchell, A.F. Sarofim, and L.A. Clomburg, (1980) "Experimental and numerical investigation of confined laminar diffusion flames," *Combustion and Flame*, vol. 3, 1980, pp. 227 -244.